JOURNAL OF ELECTROMAGNETIC ENGINEERING AND SCIENCE, VOL. 16, NO. 2, 126~133, APR. 2016

http://dx.doi.org/10.5515/JKIEES.2016.16.2.126
ISSN 2234-8395 (Online) · ISSN 2234-8409 (Print)

Analysis of Efficiencies for Multiple-Input Multiple-Output Wireless Power Transfer Systems

Sejin Kim · Bomson Lee*

Abstract

Wireless power transfer (WPT) efficiencies for multiple-input multiple-output (MIMO) systems are formulated with a goal of achieving their maximums using Z matrices. The maximum efficiencies for any arbitrarily given configurations are obtained using optimum loads, which can be determined numerically through adequate optimization procedures in general. For some simpler special cases (single-input single-output, single-input multiple-output, and multiple-input single-output) of the MIMO systems, the efficiencies and optimum loads to maximize them can be obtained using closed-form expressions. These closed-form solutions give us more physical insight into the given WPT problem. These efficiencies are evaluated theoretically based on the presented formulation and also verified with comparisons with circuit- and EM-simulation results. They are shown to lead to a good agreement. This work may be useful for construction of the wireless Internet of Things, especially employed with energy autonomy.

Key Words: Coupling Coefficient, Optimum Load Resistance, Transfer Efficiency, Wireless Power Transfer, Z Matrix.

I. Introduction

Recently, the wireless power transfer (WPT) technology has become more important, and products related to single-input single-output (SISO) WPT systems have been globally commercialized with the example of wireless charging pads [1]. To expand the WPT market, regulatory issues regarding WPT commercialization and standardization are being finalized [2]. The WPT systems with multiple transmitters or multiple receivers have also been studied [3–5]. In [3], multiple-input single-output (MISO) WPT systems were investigated using closed-form solutions for the maximum WPT efficiencies. An analysis of the WPT efficiencies considering the multiple-output system was provided in [4]. Multiple-input multiple-output (MIMO) WPT systems including a repeater with a misalignment angle were examined in [5].

Still, there are many problems left in WPT systems, such as low efficiency, realization, stability, adaptability to mobility, EMI /EMC/EMF, and so on. In this paper, the WPT problem for general MIMO systems is formulated to achieve maximum efficiencies based on optimum loads. The maximum efficiencies of the systems can be obtained systematically for any number of transmitters and receivers. With this formulation, the optimum loads for maximum efficiencies can always be found at least numerically through a proper systematic optimization process. For some special cases such as SISO, SIMO, and MISO, closed-form expressions for the efficiencies and optimum loads for maximum efficiencies are derived and examined with various examples. The validity of circuit- and EM-simulated efficiencies are compared with the theoretical efficiencies.

Manuscript received January 4, 2016 ; Revised March 4, 2016 ; Accepted April 4, 2016. (ID No. 20160104-001J)
Department of Electronic and Radio Engineering, Kyung Hee University, Yongin, Korea.
*Corresponding Author: Bomson Lee (e-mail: bomson@khu.ac.kr)

II. MIMO Wireless Power Transfer System

Fig. 1 shows a WPT system consisting of transmitters with a number of M and receivers with a number of N. They are assumed to be made of loops that have some inductances L. Each loop is loaded with a capacitor for resonance at a specific angular frequency ω_0. Then, the Z matrix for the WPT system is given by

$$\begin{bmatrix} V_1 \\ \cdots \\ V_M \\ 0 \\ \cdots \\ 0 \end{bmatrix} = \begin{bmatrix} Z_{11} & \cdots & Z_{1M} & \cdots & Z_{1,M+N} \\ \cdots & & & & \cdots \\ Z_{M,1} & & & & Z_{M,M+N} \\ Z_{M+1,1} & & & & Z_{M+1,M+N} \\ \cdots & & & & \cdots \\ Z_{M+N,1} & \cdots & Z_{1M} & \cdots & Z_{M+N,M+N} \end{bmatrix} \begin{bmatrix} I_1 \\ \cdots \\ I_M \\ I_{M+1} \\ \cdots \\ I_{M+N} \end{bmatrix}. \quad (1)$$

In (1), the elements in the column matrix $[V]$ are the supplied voltages. The supplied voltages of the receiving loops are assumed to be zero. The diagonal and off-diagonal elements of the Z matrix as a function of angular frequency ω are expressed as

$$Z_{mm} = R_m + j\omega_0 L_m \left(\frac{\omega}{\omega_0} - \frac{\omega_0}{\omega} \right) \quad \text{for } m = 1, 2, \cdots, M$$

$$Z_{mn} = R_n + R_{Ln} + j\omega_0 L_n \left(\frac{\omega}{\omega_0} - \frac{\omega_0}{\omega} \right) \quad \text{for } n = M+1, \cdots, M+N \quad (2)$$

and

$$Z_{mn} = -j\omega k_{mn} \sqrt{L_m L_n} \ (m \neq n) \ \text{for} \ m, n = 1, 2, \cdots, M+N, \quad (3)$$

respectively. In (2), R_m (m = 1, 2, ⋯, M + N) is the loss resistance of each loop, and R_{Ln} ($n = M+1, M+2, \cdots, M+N$) is the load resistance of each receiver. In (3), k_{mn} is the coupling coefficient [6].

At the resonant angular frequency (ω_0), the diagonal and off-diagonal elements in [Z] are shown to become purely resistive and purely imaginary, respectively. The current is determined by $[I] = [Z]^{-1}[V]$. Then, the total input power and the received power at n^{th} receiver are readily obtained by

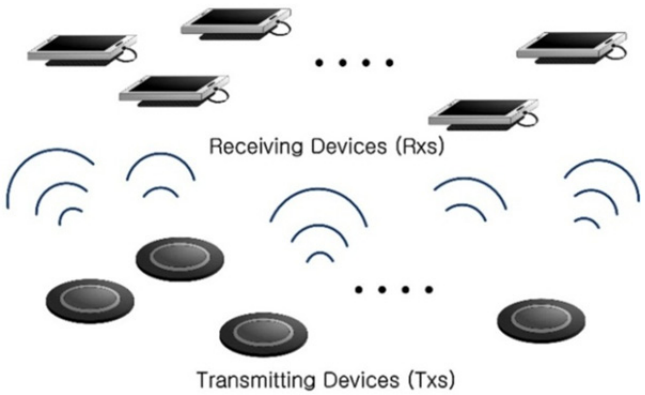

Fig. 1. Typical configuration of a MIMO WPT system.

$$P_{in} = \sum_{m=1}^{M} \frac{1}{2} \mathrm{Re}\left[V_m I_m^* \right] \quad (4)$$

and

$$P_{Ln} = \frac{1}{2} R_{Ln} |I_n|^2 \ (n = M+1, M+2, \cdots, M+N). \quad (5)$$

The WPT efficiencies for the n^{th} receiver and the whole receivers are simply given by

$$\eta_n = \frac{P_{Ln}}{P_{in}} \ (n = M+1, M+2, \cdots, M+N) \quad (6)$$

and

$$\eta = \sum_{n=M+1}^{M+N} \eta_n, \quad (7)$$

respectively. Based on this formulation, the WPT efficiencies for any MIMO configurations with arbitrary loads R_{Ln} ($n = M+1$, ⋯, $M+N$) can be evaluated. For design problems to maximize (6) or (7), the solutions for R_{Ln} ($n = M+1$, ⋯, $M+N$) can be obtained at least numerically using Genetic Algorithm (evolutionary algorithm), which is a proper optimization algorithm. For some special cases of MIMO WPT systems such as SISO, SIMO, and MISO, we also try to analyze them analytically if possible.

When the number of transmitting and receiving loops is 1 ($M = N = 1$, SISO), all solutions are already well- known but are repeated here for readers' convenience. The transmitted power P_{in}, received power P_L, and the WPT efficiency are given by [7]

$$P_{in} = \frac{1}{2} \mathrm{Re}\left[V I_1^* \right] = \frac{|V_1|^2}{2R_1} \cdot \frac{1+\beta}{1+\beta+F^2}, \quad (8)$$

$$P_L = \frac{1}{2} |I_2|^2 R_L = \frac{|V_1|^2}{2R_1} \cdot \frac{\beta F^2}{\left(1+\beta+F^2\right)^2}, \quad (9)$$

and

$$\eta(F, \beta) = \frac{P_L}{P_{in}} = \frac{\beta F^2}{(1+\beta)\left(1+\beta+F^2\right)}, \quad (10)$$

respectively, where the normalized load β ($= R_L/R_2$) and the figure of merit F ($= kQ$) are independent variables to determine the efficiencies. Q is the geometric mean of Q_1 and Q_2 $\left(Q = \sqrt{Q_1 Q_2}\right)$, and each is given by $\omega_0 L/R$. It is known that (10) can also be expressed as

$$\eta(F, b) = \frac{F^2}{\left(1 + b\sqrt{1+F^2}\right)\left(1 + \frac{1}{b}\sqrt{1+F^2}\right)} \quad (11)$$

where b ($= R_L/R_{L,opt} = \beta / \beta_{opt}$) is the normalized load resistance referenced to the optimum $R_{L,opt}$ with which the maximum efficiency is achieved. β_{opt} is the normalized optimum load resistance for maximum efficiency, given by $\beta_{opt} = R_{L,opt}/R_2 = \sqrt{1+F^2}$ [6, 7]. When $b = 1$, the efficiency in (11) becomes maximum. When b is greater or less than 1, the two-loop WPT system becomes under-coupled or over-coupled, respectively, and the efficiencies decrease. It is interesting to observe that as F ($= kQ$) becomes smaller, $R_{L,opt}$ also becomes smaller. The condition of $R_{L,opt} = R_2$ when $F = 0$ (two loops placed far apart) reminds us of the condition of the maximum received power of an Rx antenna in the far field. It is also notable that even though the role of Tx and Rx loops are interchanged, the efficiency remains the same with a similar use of the optimum load.

III. Analysis of Wireless Power Transfer for Special Cases

1. Single-input Multiple-Output System ($M = 1$, $N = 2$)

Fig. 2 shows a WPT system consisting of one transmitter and two receivers. The center positions of each loop are assumed to be at (0, 0, 0), (0, $-h$, v), and (0, h, v), respectively. We can analyze the system using a simple 3×3 Z matrix using (1)–(3).

When the distance between the two receiving loops is large, the coupling coefficient k_{32} is negligibly small and can be assumed to be zero. For this case, the WPT efficiency of each loop can be expressed as

$$\eta_2 = \frac{\beta_2}{(1+\beta_2)} \cdot \frac{F_{21}^2}{1+\beta_2+F_{21}^2+\dfrac{F_{31}^2}{(1+\beta_3)}} \tag{12}$$

and

$$\eta_3 = \frac{\beta_3}{(1+\beta_3)} \cdot \frac{F_{31}^2}{1+\beta_3+F_{31}^2+\dfrac{F_{21}^2}{(1+\beta_2)}}, \tag{13}$$

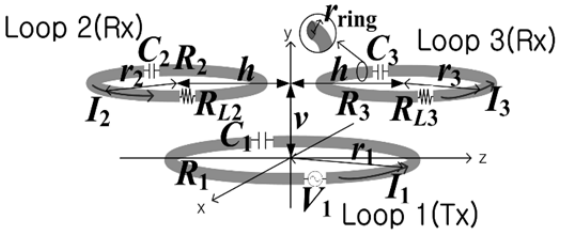

Fig. 2. A SIMO system ($M = 1$, $N = 2$) with two horizontally placed receivers. Each loop is located at (0, 0, 0), (0, $-h$, v), and (0, h, v).

where F_{n1} is the figure of merit defined by $F_{n1} = k_{n1}\sqrt{Q_n Q_1}$. Q_n is the quality factor given by $\omega_0 L_n/R_n$, and β_n is the normalized load resistance defined by R_{Ln}/R_n. The total WPT efficiency η is the sum of (12) and (13) as defined in (7). The normalized optimum load resistances $\beta_{2,opt}$ and $\beta_{3,opt}$ with which (12) and (13) are maximized can be shown to be given by

$$\beta_{2,opt} = \frac{R_{L2,opt}}{R_2} = \sqrt{\left(1+F_{21}^2+\frac{F_{31}^2}{1+\beta_3}\right)\Big/\left(1+\frac{F_{31}^2}{1+\beta_3}\right)} \tag{14}$$

and

$$\beta_{3,opt} = \frac{R_{L3,opt}}{R_3} = \sqrt{\left(1+F_{31}^2+\frac{F_{21}^2}{1+\beta_2}\right)\Big/\left(1+\frac{F_{21}^2}{1+\beta_2}\right)}, \tag{15}$$

respectively. When $\beta_3 \to \infty$ (open) in (14), loop 3 becomes inactive (under-coupled limit), $\beta_{2,opt} = \sqrt{1+F_{21}^2}$ (normalized optimum load for the SISO WPT system). When $\beta_3 \to 0$ (short, over-coupled limit), $\beta_{2,opt} = \sqrt{\left(1+F_{21}^2+F_{31}^2\right)/\left(1+F_{31}^2\right)}$. The solution of R_{L2} and R_{L3} for the maximum η ($= \eta_2 + \eta_3$) may also be numerically determined with GA.

All the efficiencies and optimum loads evaluated and presented in this paper have been checked between the GA results based on (2)–(7) and circuit/EM-simulation results. The efficiencies and optimum loads have been found to be always in good agreement.

Fig. 3(a) and (b) show the maximum WPT efficiencies and the optimum load resistances for the case described in Fig. 2. The resonant frequency is 6.78 MHz, $r_1 = 15$ cm, $r_2 = r_3 = 5$ cm, and $r_{ring} = 0.2$ cm. The Q-factors for the loops with $r_1 = 15$ cm and $r_2 = r_3 = 5$ cm are about 730 and 560, respectively.

In Fig. 3(a), the efficiency η ($= \eta_2 + \eta_3$) are plotted as a function of h for $v = 3$ cm, 5 cm, and 7.5 cm. Besides, for the purpose of comparison, we have also plotted η_2 when $v = 3$ cm without loop 3. It is shown that when h is smaller than roughly the radius of the Tx loop 1 (15 cm), η_2 without loop 3 is greater than 90%, and it is almost the same as the total efficiency η ($= \eta_2 + \eta_3$) with both loop 2 and loop 3 symmetrically placed.

This means that when the Rx loops are properly placed in symmetry relative to the Tx loop, the nearly 100% efficiency can be shared by the receiving loops. When h is roughly between 17 cm and 20 cm, the efficiencies drastically drop to zero. These zero-efficiency phenomena occur at positions where the upward magnetic flux lines crossing a receiving loop change their directions and fall down into the loop again such that the net magnetic flux crossing the loop is zero. This corresponds to the zero-coupling coefficients (k).

Beyond the zero-efficiency (or the zero-coupling coefficient) positions, the net magnetic flux lines on the receiving loops go

downward (the negative k changes only the direction of currents on the receiving loops), and the efficiencies are shown to increase to about 80% to 90% , but decrease again as h becomes large.

In Fig. 3(b), we show $R_{L2,opt}$ (= $R_{L3,opt}$) as a function of v and h. When the distance between the Tx and Rx loops becomes large, $R_{L,opt}$ may become too small to be realized. This can be handled with a multi-turn Rx loop or an additional feeding loop or matching circuit [8–10] depending on the system requirements.

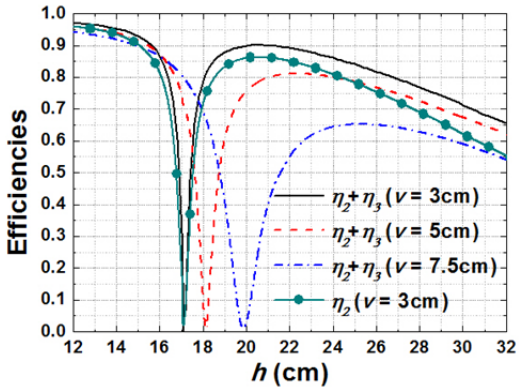

(a)

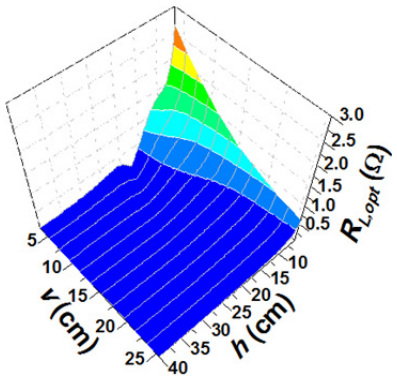

(b)

Fig. 3. WPT efficiencies and optimum load resistances at 6.78 MHz (r_1 = 15 cm, r_2 = r_3 = 5 cm, r_{ring} = 0.2 cm, Q_1 = 730, Q_2 = Q_3 = 560). (a) WPT efficiencies depending on h, (b) optimum load resistance $R_{L2,opt}$ (= $R_{L3,opt}$) to maximize the total efficiency η (= $\eta_2 + \eta_3$), as a function of v and h.

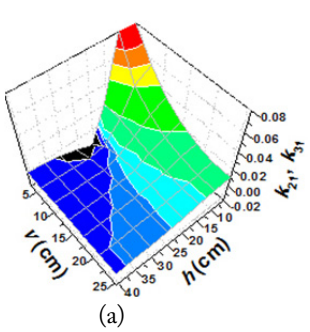

(a)

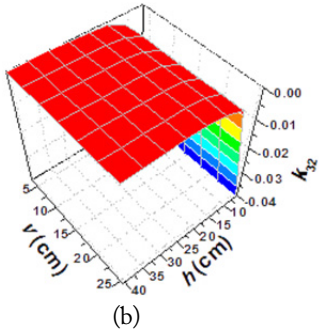

(b)

Fig. 4. Coupling coefficients at 6.78 MHz as a function of h and v (r_1 = 15 cm, r_2 = r_3 = 5 cm, r_{ring} = 0.2 cm). (a) k_{21}, k_{31} and (b) k_{32}.

Fig. 4 shows the coupling coefficients k_{21}, k_{31}, and k_{32} depending on the distances v and h based on the same system configuration as described in Fig. 3. The coupling coefficients k's were extracted based on [6]. These extracted coupling coefficients were checked to be the same as those obtained by [11]. As explained with Fig. 3(a), k_{21} and k_{31} (the coupling coefficients between the transmitting and receiving loops) are shown to be negative, zero, and positive depending on the loop 1 and loop 2 (or loop 3) positions. Due to the particular placements of loop 2 and loop 3 on a horizontal plane, k_{32} in Fig. 4(b) is always negative.

Fig. 5 shows the coupling coefficients k_{21} (= k_{31}), k_{32}, and $|k_{32}/k_{21}|$ depending on the distance h with the fixed v of 3 cm based on the system configuration as described in Fig. 4. By evaluating $|k_{32}/k_{21}|$ depending on the horizontal separation h, we can determine the condition where k_{32} may be ignored. We can see that since $|k_{32}/k_{21}|$ is very small (less than 0.3) when h > 10 cm and v = 3 cm, the solutions in (12)−(15) are more accurate in this region.

2. Multiple-Input Single-Output System (M = 2, N = 1)

Fig. 6 shows a MISO configuration consisting two transmitters and one receiver. The center positions of each loop are (0, −h, 0), (0, h, 0), and (0, 0, v), respectively.

Fig. 7 shows the maximum WPT efficiencies for the system-

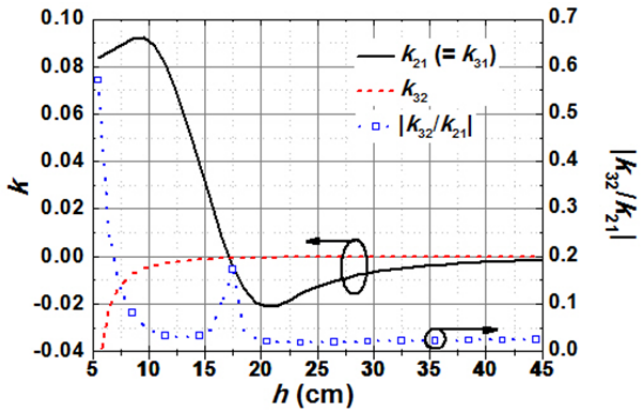

Fig. 5. k_{21}, k_{31} and k_{32} and $|k_{32}/k_{21}|$ at 6.78 MHz as a function of h (r_1 = 15 cm, r_2 = r_3 = 5 cm, r_{ring} = 0.2 cm, v = 3 cm).

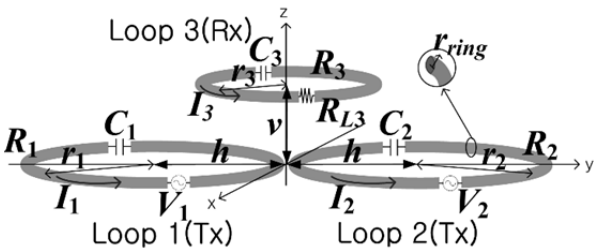

Fig. 6. A MISO system (M=2, N=1) with two horizontally placed transmitters. Each loop is located at (0, −h, 0), (0, h, 0), and (0, 0, v).

described in Fig. 6. The resonant frequency is 6.78 MHz, $V_1 = V_2$, $r_1 = r_2 = 15$ cm, $r_3 = 5$ cm, and $r_{ring} = 0.2$ cm. The Q-factors for the loops with $r_1 = r_2 = 15$ cm and $r_3 = 5$ cm are about 730 and 560, respectively.

In Fig. 7, the maximum efficiency η_3 are plotted as a function of h for $v = 3$ cm, 5 cm, and 7.5 cm. Besides, for the purpose of comparison, we have also plotted η_3 without loop 2 when $v = 3$ cm. It is shown that when h is about 16 cm, η_3 without loop 2 is approximately 90%, but η_3 with loop 2 is somewhat less than 90%. When h is roughly between 17 cm and 20 cm, the efficiencies drastically drop to zero. Beyond the zero-efficiency (or the zero-coupling coefficient) positions, the efficiencies are shown to increase to about 55% to 85%, but decrease again as h becomes large.

Fig. 8 shows the coupling coefficients k_{21}, k_{31}, and k_{32} depending on the distances v and h under the same conditions as described in Fig. 7.

Fig. 9 shows a MISO system ($M = 2$, $N = 1$) with two vertically placed transmitters. The center positions of each loop are $(0, 0, -v)$, $(0, 0, v)$, and $(0, 0, 0)$, respectively.

Fig. 10(a) and (b) show the WPT efficiency η_3 and coupling coefficients for the case described in Fig. 9. The resonant frequency is 6.78 MHz, $V_1 = V_2$, $r_1 = r_2 = 15$ cm, $r_3 = 5$ cm, and $r_{ring} = 0.2$ cm. The Q-factors for the loops with $r_1 = r_2 = 15$ cm and $r_3 = 5$ cm are about 730 and 560, respectively. In Fig. 10(a), the maximum efficiencies η_3 with and without loop 2 are plotted as a function of v. For the purpose of comparison, we have also

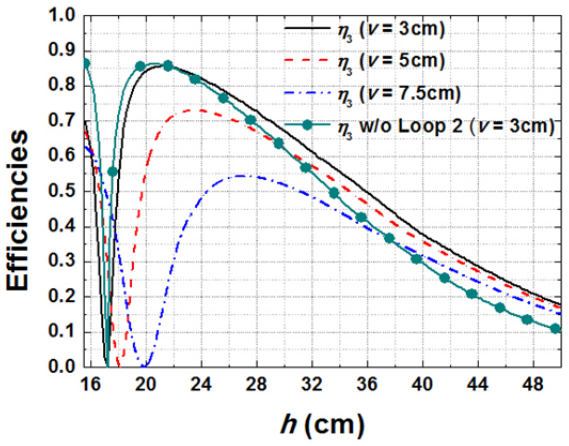

Fig. 7. WPT efficiencies at 6.78 MHz with $V_1 = V_2$ ($r_1 = r_2 = 15$ cm, $r_3 = 5$ cm, $r_{ring} = 0.2$ cm, $Q_1 = Q_2 = 730$, $Q_3 = 560$).

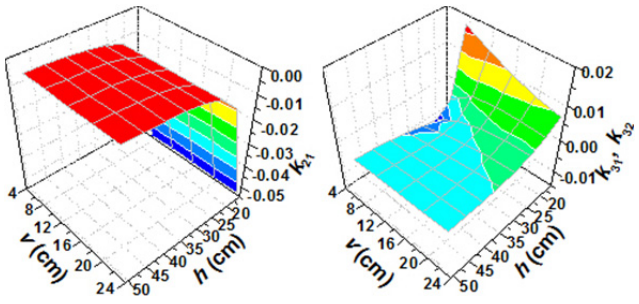

(a) (b)

Fig. 8. Coupling coefficients at 6.78 MHz as function of h and v ($r_1 = r_2 = 15$ cm, $r_3 = 5$ cm, $r_{ring} = 0.2$ cm, $Q_1 = Q_2 = 730$, $Q_3 = 560$). (a) k_{21} and (b) k_{31}, k_{32}.

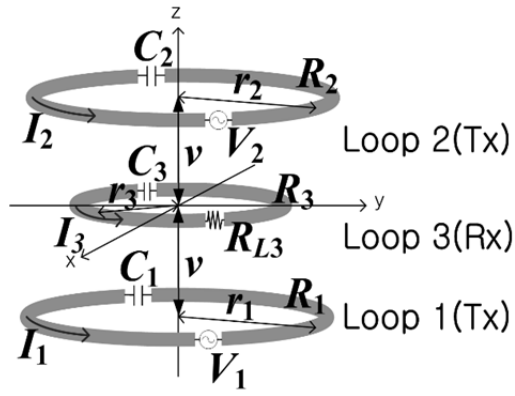

Fig. 9. A MISO system ($M = 2$, $N = 1$) with two vertically placed transmitters. Each loop is located vertically at $(0, 0, -v)$, $(0, 0, v)$ and $(0, 0, 0)$.

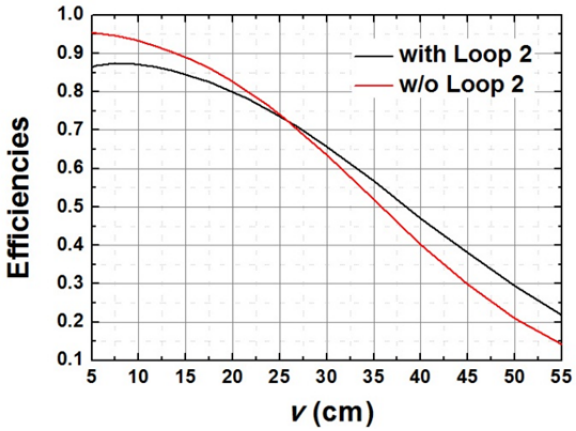

(a)

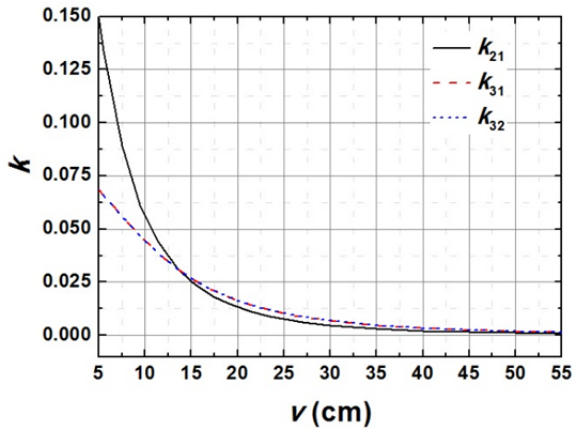

(b)

Fig. 10. WPT efficiencies η_3 and coupling coefficients k_{21}, k_{31}, and k_{32} at 6.78 MHz with $V_1 = V_2$ depending on v ($r_1 = r_2 = 15$ cm, $r_3 = 5$ cm, $r_{ring} = 0.2$ cm, $Q_1 = Q_2 = 730$, $Q_3 = 560$). (a) WPT efficiencies, (b) k_{21}, k_{31} and k_{32}.

plotted η_3 without loop 2.

When v is smaller than 26 cm, η_3 without loop 2 is somewhat greater than η_3 with loop 2. When v is larger than 26 cm, the opposite is true. As v increases, the benefit of using two Tx loops is shown to be more significant.

3. Multiple-Input Multiple-Output System ($M=2$, $N=2$)

Fig. 11 shows a MIMO system ($M = 2$, $N = 2$). Performances of this system can also be analyzed using the formulation (1)–(7).

Fig. 12(a) and (b) show the WPT efficiencies and the optimum load resistances for the case described in Fig. 10. The

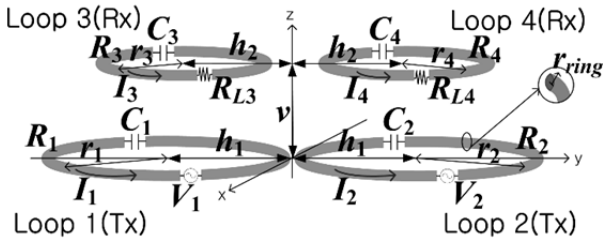

Fig. 11. A MIMO system ($M=2$, $N=2$) with two horizontally placed transmitters and receivers. Each loop is located at $(0, -h_1, 0)$, $(0, h_1, 0)$, $(0, -h_2, v)$, and $(0, h_2, v)$.

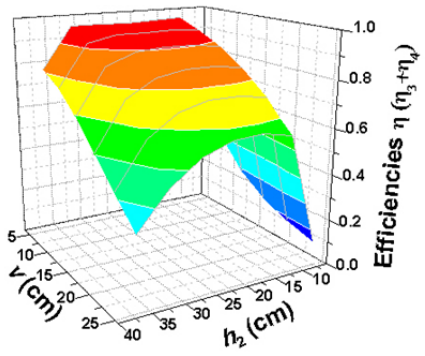

(a)

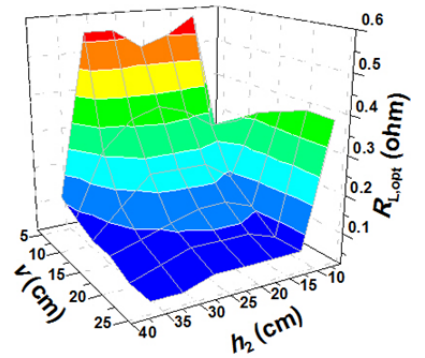

(b)

Fig. 12. WPT efficiencies and optimum load resistances at 6.78 MHz with $V_1 = V_2$ depending on h_2 and v ($r_1 = r_2 = 15$ cm, $r_3 = r_4 = 5$ cm, $r_{ring} = 0.2$ cm, $h_1 = 20$ cm, $Q_1 = Q_2 = 730$, $Q_3 = Q_4 = 560$). (a) WPT efficiencies η ($= \eta_3 + \eta_4$), (b) optimum load resistance $R_{L3,opt}$ ($= R_{L4,opt}$).

resonant frequency is 6.78 MHz, $V_1 = V_2$, $r_1 = r_2 = 15$ cm, $r_3 = r_4 = 5$ cm, $r_{ring} = 0.2$ cm, and $h_1 = 20$ cm. The Q-factors for the loops with $r_1 = r_2 = 15$ cm and $r_3 = r_4 = 5$ cm are about 730 and 560, respectively.

In Fig. 12(a), η ($= \eta_3 + \eta_4$) are plotted as a function of v and h_2. It is shown that when 5 cm $\leq v \leq$ 15 cm and 10 cm $\leq h_2 \leq$ 30 cm, η ($= \eta_3 + \eta_4$) is well above 90%. In Fig. 12(b), $R_{L,opt}$ is shown to be about 0.5 Ω when v is 5 cm and 30 cm $\leq h_2 \leq$ 35 cm.

Fig. 13 shows the coupling coefficients k_{21}, k_{31}, k_{32}, k_{41}, k_{42}, and k_{43} depending on the distances v and h_2 under the same conditions as described in Fig. 12. In Fig. 13(a), k_{21} (the coupling coefficients between the transmitting loops) is about −0.0014. In Fig. 13(c), k_{41} and k_{32} (the coupling coefficients between the transmitting and receiving loops that are located diagonally) are shown to be negative, zero, and positive, depending on the loop positions.

Since the MIMO WPT systems are considered to be a natural extension of the SISO system, the overall WPT system efficiencies have been found to be well above 90% when the distances between the TX and Rx loops are roughly less than the radius of the Tx loops.

Fig. 14 shows a MIMO system ($M = 2$, $N = 2$). Performances of this system can also be analyzed using (1)–(7).

Fig. 15 shows the WPT efficiencies for the case described with all loops (MIMO) or without loop 2 and loop 4 (SISO) in Fig. 14. The resonant frequency is 6.78 MHz, $V_1 = V_2$, $r_1 = r_2 = r_3 = r_4 = 5$ cm, $r_{ring} = 0.2$ cm. The Q-factors for the loops with $r_1 = r_2 = r_3 = r_4 = 5$ cm are about 560.

In Fig. 15, η ($= \eta_3 + \eta_4$) (MIMO) and η_3 (SISO) are plotted

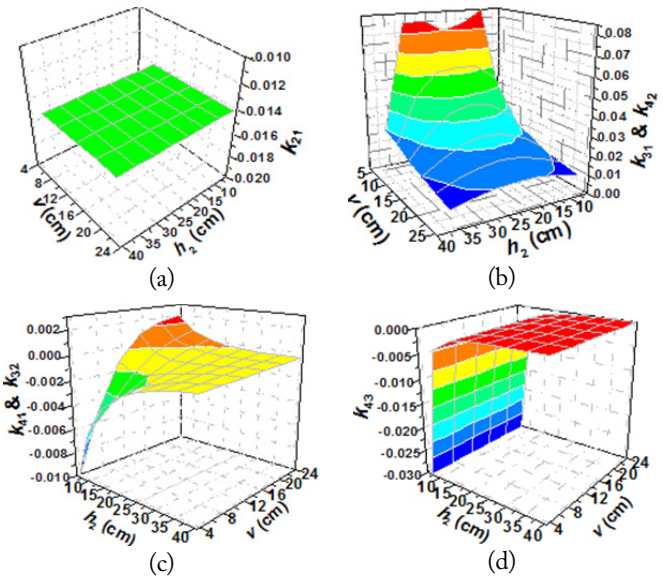

(a) (b) (c) (d)

Fig. 13. Coupling coefficients at 6.78 MHz with $V_1 = V_2$ as function of v and h_2 ($r_1 = r_2 = 15$ cm, $r_3 = r_4 = 5$ cm, $r_{ring} = 0.2$ cm, $h_1 = 20$ cm, $Q_1 = Q_2 = 730$, $Q_3 = Q_4 = 560$). (a) k_{21}, (b) k_{31}, k_{32}, (c) k_{41}, k_{42}, and (d) k_{43}.

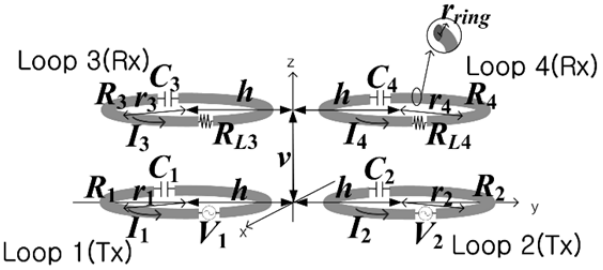

Fig. 14. A MIMO system ($M=2$, $N=2$) with two horizontally placed transmitters and receivers. Each loop is located at $(0, -h, 0)$, $(0, h, 0)$, $(0, -h, v)$, and $(0, h, v)$.

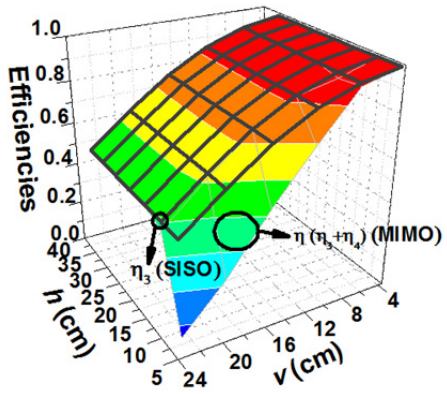

Fig. 15. WPT efficiencies and optimum load resistances at 6.78 MHz with $V_1=V_2$ depending on h and v ($r_1=r_2=r_3=r_4=5$ cm, $r_{ring}=0.2$ cm, $Q_1=Q_2=Q_3=Q_4=560$), WPT efficiencies.

as a function of v and h. It is shown that when 4 cm $\leq v \leq$ 8 cm, η $(=\eta_3+\eta_4)$ (MIMO) and η_3 (SISO) are well above 90%. It is shown that η $(=\eta_3+\eta_4)$ (MIMO) becomes smaller as the vertical separation v becomes larger. η $(=\eta_3+\eta_4)$ (MIMO) is about 0.1–0.6 when 5 cm $\leq h \leq$ 10 cm and 14 cm $\leq v \leq$ 24 cm. It becomes smaller than η_3 (SISO) since η $(=\eta_3+\eta_4)$ (MIMO) is affected by the coupling of the four loops. This implies that it is more effective to use a SISO system when 5 cm $\leq h \leq$ 10 cm than to use a MIMO system.

Although the EM simulation results have been analyzed and discussed up to $M=2$ and $N=2$ systems, MIMO WPT systems with more Tx and Rx loops are expected to have similar performance behaviors.

In particular, for the WPT system with $M=1$ and arbitrary N, the efficiencies of the Rx loops have been found to be shared among them, and the total efficiency can be engineered up to 1 depending on the system configurations.

IV. Conclusion

We formulated the MIMO WPT systems in terms of transfer efficiencies for each receiver and the whole receivers. The optimum loads of the receivers for the maximum WPT efficiencies have been shown to be found at least numerically based on the formulation. For some typical special cases of SISO, MISO, and SIMO system have been analyzed using circuit- and EM-simulations together with the derived closed-form solutions. In particular, the SIMO system has been shown to be effective in that the near 100% efficiency can be shared by the receiving loops. The derived closed-form solutions have been demonstrated to give us plentiful physical insight for the systems. The results of this paper may be useful to construct WPT systems for Internet of Things requiring sensors with energy autonomy without batteries.

This work was supported by the National Research Foundation of Korea (NRF) grant funded by the Korea government (MSIP) (No. NRF-2013-R1A2A2A01015202).

References

[1] B. K. Chung and H. T. Chuah, "Design and construction of a multipurpose wideband anechoic chamber," *IEEE Antennas and Propagation Magazine*, vol. 45, no. 6, pp. 41–47, 2003.

[2] A. Kazemzadeh and A. Karlsson, "Capacitive circuit method for fast and efficient design of wideband radar absorbers," *IEEE Transactions on Antennas and Propagation*, vol. 57, no. 8, pp. 2307–2314, 2009.

[3] J. Tak, Y. Lee, and J. Choi, "Design of a metamaterial absorber for ISM applications," *Journal of Electromagnetic Engineering and Science*, vol. 13, no. 1, pp. 1–7, 2013.

[4] X. Shen, T. Cui, J. Zhao, H, Ma. W. Jiang, and H. Li, "Polarization independent wide-angle triple-band metamaterial absorber," *Optics Express*, vol. 19, no. 10, pp. 9401–9407, 2011.

[5] H. Li, L. H. Yuan, B. Zhou, X. P. Shen, Q. Cheng, and T. J. Cui, "Ultrathin multiband gigahertz metamaterial absorbers," *Journal of Applied Physics*, vol. 110, no. 1, article no. 014909, 2011.

[6] R. L. Fante and M. T. McCormack, "Reflection properties of the Salisbury screen," *IEEE Transactions on Antennas Propagation*, vol. 36, no.10, pp. 1443–1454, 1988.

[7] A. P. Sohrab and Z. Atlasbaf, "A circuit analog absorber with optimum thickness and response in X-band," *IEEE Antennas and Wireless Propagation Letters*, vol. 12, pp. 276–279, 2013.

[8] G. R. Zhang, P. H. Zhou, H. B. Zhang, L. B. Zhang, J. L. Xie, and L. J. Deng, "Analysis and design of triple-band high-impedance surface absorber with periodic diversified impedance," *Journal of Applied Physics*, vol. 114, no. 16,

article no. 164103, 2013.

[9] B. K. Kim and B. Lee, "Design of metamaterial-inspired wideband absorber at X-band adopting trumpet structures," *Journal of Electromagnetic Engineering and Science*, vol. 14, no. 3, pp. 314–316, 2014.

[10] G. Kim and B. Lee, "Design of wideband absorbers using RLC screen," *Electronics Letters*, vol. 51, no. 11, pp. 834–836, 2015.

[11] B. K. Kim and B. Lee, "Wideband absorber at X-band adoption resistive trumpet structures," *Electronics Letters*, vol. 50, no. 25, pp. 1957–1959, 2014.

[12] F. Costa, S. Genovesi, A. Monorchio, and G. Manara, "Low-cost metamaterial absorbers for sub-GHz wireless system," *IEEE Antennas and Wireless Propagation Letters*, vol.13, pp. 27–30, 2014.

[13] H. Zhang, P. Zhou, H. Lu, Y. Xu, J. Xie, and L. Deng, "Soft-magnetic-film based metamaterial absorber" *Electronics Letters*, vol. 48, no. 8, pp. 435–437, 2012.

[14] S. Ghosh and K. V. Srivastava, "An equivalent circuit model of FSS-based metamaterial absorber using coupled line theory," *IEEE Antennas and Wireless Propagation Letters*, vol. 14, pp. 511–514, 2015.

[15] Y. Cheng, H. Yang, and N. Wu, "Perfect metamaterial absorber based on a split-ring-cross resonator," *Applied Physics A*, vol. 102, no. 1, pp. 99–103, 2011.

Sejin Kim

received the B.S. degree in Electronics and Radio Engineering from Kyung Hee University, Yong-in, Korea, in 2015. She is currently working toward a master's degree in Electronics and Radio Engineering at Kyung Hee University. Her fields of research include wireless power transmission system, passive devices, small antenna, RFID reader antennas, and metamaterials.

Bomson Lee

received a B.S. degree in Electrical Engineering from Seoul National University, Seoul, Korea, in 1982, and M.S. and Ph.D. degrees in Electrical Engineering from the University of Nebraska, Lincoln, NE, U.S.A., in 1991 and 1995, respectively. From 1982 to 1988, he was with the Hyundai Engineering Company Ltd., Seoul, Korea. In 1995, he joined the faculty at Kyung Hee University, where he is currently a professor with the Department of Electronics and Radio Engineering. He was an editor-in-chief of the Journal of the Korean Institute of Electromagnetic Engineering and Science in 2010. He is an executive director (Project) in KIEES (Korea Institute of Electromagnetic Engineering & Science). Since 2015, he has been a vice-chairman, Korea Institute of Electromagnetic Engineering and Science (KIEES). His research activities include microwave antennas, RF identification (RFID) tags, microwave passive devices, wireless power transmission, and metamaterials.